DELAMINATION OF THIN FILMS

Henrik Myhre Jensen
Department of Building Technology and Structural Engineering
Aalborg University, Sohngaardsholmsvej 57
DK-9000 Aalborg, DENMARK
hmj@bt.aau.dk

Summary

The paper presents an overview of some recent results involved in the delamination of thin films.

Spontaneous delamination of thin films from a substrate may be initiated at edges corners or at large flaws at the interface. Effects of curvature of the substrate and corners in the substrate on buckling-driven delamination of thin films in compression are analysed. In particular an analysis of buckling-driven delamination of a thin film on a spherical substrate has been carried out. The effects of the substrate having a double curvature compared to previous studies of delamination on cylindrical substrates turns out to be non-trivial: In addition to the effect of the shape of the substrate, a new non-dimensional geometrical parameter enters the conditions for steady-state delamination. It is shown that for a certain range of delamination widths, this additional geometrical parameter has only minor influence on the conditions for steady-state delamination. Furthermore, the shape of the substrate has profound influence especially on initiation of delamination growth.

Details in the morphology of buckling-driven delamination and in particular possible causes of the so-called telephone cord blister are discussed. Conditions for steady-state growth of buckling-driven delamination in thin film systems can be calculated by a simplified method where details around the growing front are not required. The simplified method relies upon estimates of the phase angle of loading along the propagating front of delamination and the accuracy of these estimates is investigated by comparing with finite element calculations of the fracture mechanics parameters along the growing front.

Interface fracture mechanics

The relations between the combined mode I/II and the mode III energy release rates and the normal membrane force, N, an effective moment, M, and shear membrane force, T, in the thin film (of thickness h) along the crack front are given by (Jensen et al. [1])

$$G = G_{I/II} + G_{III} \quad , \quad G_{I/II} = \frac{1-\nu^2}{2Eh^3}\left(12M^2+h^2N^2\right) \quad , \quad G_{III} = \frac{1+\nu}{Eh}T^2 \tag{1}$$

where E and ν are the Young's modulus and the Poisson's ratio for the film, respectively. A separation of the energy release rate into mode I, II and III components follow from the definitions of the phase angles of loading ψ and ϕ introduced in [1] and Suo and Hutchinson [2]

$$\tan\psi = \frac{\mathrm{Im}\left((K_I + iK_{II})L^{i\varepsilon}\right)}{\mathrm{Re}\left((K_I + iK_{II})L^{i\varepsilon}\right)} \quad , \quad \cos\phi = \sqrt{\frac{G_{III}}{G}} \tag{2}$$

where K_I and K_{II} are the mode I and II stress intensity factors, i is the imaginary unit, L is an arbitrary reference length and ε is the bimaterial constant, which - along with the two Dundurs' parameters α_D and β_D - are given in terms of the elastic constants for the bimaterial system by the relations

$$\begin{aligned} \varepsilon &= \frac{1}{2\pi}\ln\frac{1-\beta_D}{1+\beta_D} \quad , \quad \alpha_D = \frac{\bar{E}-\bar{E}_s}{\bar{E}+\bar{E}_s} \\ 2\beta_D\left(\bar{E}+\bar{E}_s\right) &= \bar{E}\frac{1-2\nu_s}{1-\nu_s} - \bar{E}_s\frac{1-2\nu}{1-\nu} \quad , \quad \bar{E} = \frac{E}{1-\nu^2} \end{aligned} \tag{3}$$

The subscript $(\,)_s$ refers to the substrate.

The relation between the energy release rate and the stress intensity factors K_I, K_{II} and K_{III} is given by

$$G = \frac{1}{\cosh^2(\pi\varepsilon)}\frac{1}{2}\left(\frac{1}{\bar{E}}+\frac{1}{\bar{E}_s}\right)\left(K_I^2+K_{II}^2\right)+\frac{1}{2}\left(\frac{1+\nu}{E}+\frac{1+\nu_s}{E_s}\right)K_{III}^2 \tag{4}$$

By combination of (2) and (4) it can be shown that ψ and ϕ are Euler angles in a space of scaled stress intensity factors $\left(\mathrm{Re}\left((K_I + iK_{II})L^{i\varepsilon}\right), \mathrm{Im}(K_I + iK_{II})L^{i\varepsilon}, cK_{III}\right)$ as illustrated in Fig. 1. A consequence of this definition of phase angles of loading is that the Griffith fracture criterion

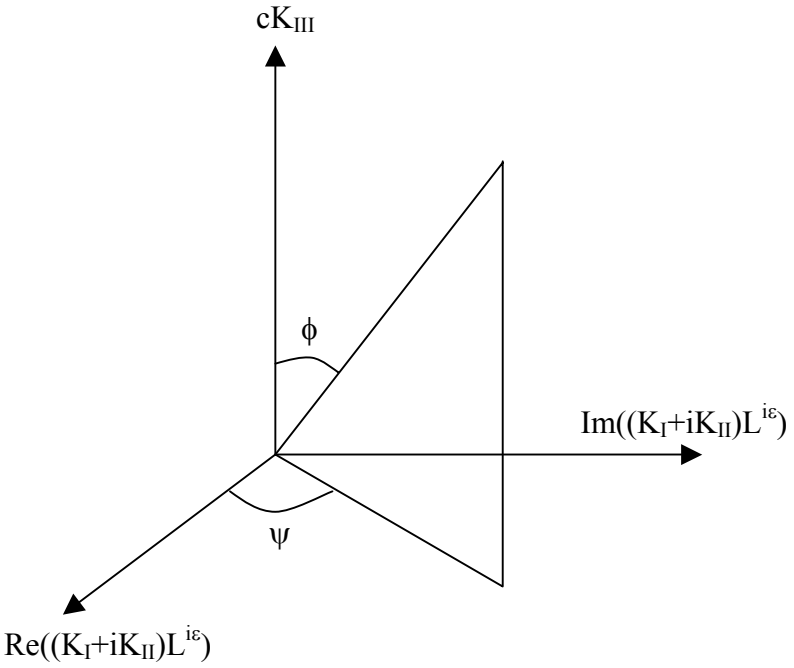

Figure 1. Phase angles of loading.

maps on a sphere in this space of scaled stress intensity factors. The factor c is

$$c = \cosh(\pi\varepsilon)\sqrt{\left(\frac{1+\nu}{E}+\frac{1+\nu_s}{E_s}\right)\left(\frac{1-\nu^2}{E}+\frac{1-\nu_s^2}{E_s}\right)^{-1}} \tag{5}$$

The asymptotic near tip stress field σ varies with distance r to the crack tip according to $\sigma \sim r^{i\varepsilon - 1/2}$ so that the stresses and displacements oscillate sufficiently close to the crack tip unless $\varepsilon = 0$. An interface fracture criterion formulated in [1] for non-oscillating singular crack tip fields is applied here in the form

$$G_I + \lambda_2 G_{II} + \lambda_3 G_{III} = G_{1c} \tag{6}$$

where λ_2 and λ_3 are parameters between 0 and 1 adjusting the relative contributions of mode II and III to the fracture criterion, and G_{1c} is the mode I interface fracture toughness.

Delamination at corners

Delamination in thin film systems at corners as sketched in Fig. 2 was analysed in Jensen [3] and Pane and Jensen [4].

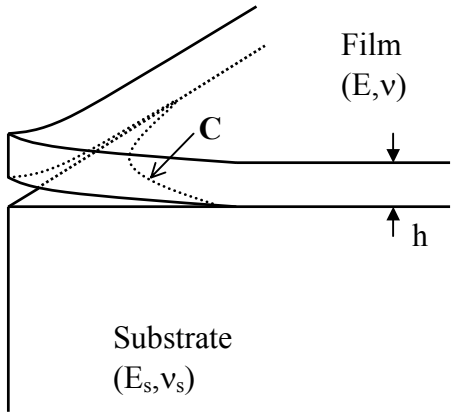

Figure 2. Delamination at a corner.

Eshelby's cut and paste technique is used in combination with a division of the problem into the solution of an outer problem for determining the stresses in the film on a scale comparable to the size of the delamination, and an inner problem where these stresses are coupled to the fracture mechanical parameters at the crack front via (6). Fig. 3 is a sketch illustrating the outer problem.

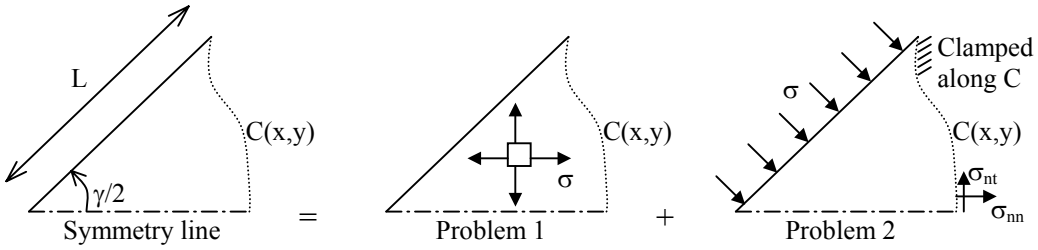

Figure 3. The outer problem is divided into sub problems 1 and 2.

The residual stresses are assumed tensile so that (6) reduces to

$$\sigma_{nn}^2 + \frac{\lambda}{1-\nu}\sigma_{nt}^2 = \sigma_c^2 = \frac{2EG_c^*}{(1-\nu^2)h} \tag{7}$$

where σ_{nn} and σ_{nt} is the effective normal and shear stress in the film at the crack front for sub problem 2 defined in Fig. 3, and where

$$\lambda = \frac{\lambda_3}{1+(\lambda_2-1)\sin^2\psi} \quad , \quad G_c^* = \frac{G_{1c}}{1+(\lambda_2-1)\sin^2\psi} \tag{8}$$

The properties of the substrate affect the fracture criterion through $\psi = \psi(\alpha_D,\beta_D)$.

The finite element method is used for calculating σ_{nn} and σ_{nt} for sub problem 2. The shape of the crack front is represented by a series of polynomials, and an iterative procedure is formulated to determine the shape so that (8) is satisfied locally along the crack front.

The stress σ_c has the interpretation of being the stress at which steady state delamination under plane strain conditions of a straight sided edge crack is possible. Delamination at corners is possible at lower stress levels and examples of delamination shapes are shown in Fig. 4.

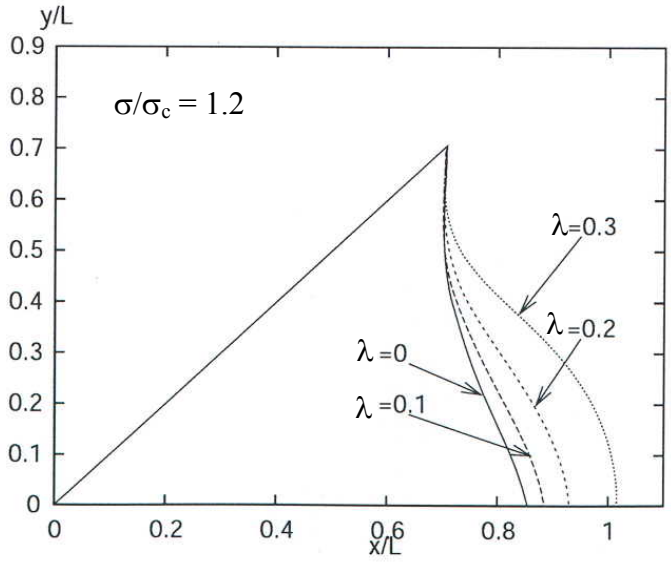

Figure 4. Predicted crack front shapes.

Effects of substrate curvature

Thin film delamination driven by buckling of the film for cases of compressive residual stresses was analysed in Hutchinson and Suo [5] for a planar system. This type of delamination propagates in a self similar fashion under steady state conditions. This allows for a simplified analysis where the energy release rate required to propagate the crack can be calculated by the difference in strain energy densities, W, of unit segments far in front of and far behind the propagating front. The accuracy of this approach was investigated in Jensen and Sheinman [6] where finite element calculations resolving details at the propagating crack front were performed.

The analysis of [5] was generalised in Hutchinson [7] to cylindrical substrates and in Sørensen and Jensen [8] to double curved substrates. The strain energy density is then given in terms of the effective membrane stress tensor $N_{\alpha\beta}$ and the curvature tensor $K_{\alpha\beta}$ as

$$W = \frac{1}{2Eh}\left[(1+\nu)N_{\alpha}^{\beta}N_{\beta}^{\alpha} - \nu N_{\alpha}^{\alpha}N_{\beta}^{\beta}\right] + \frac{Eh^3}{24(1-\nu^2)}\left[(1-\nu)K_{\alpha}^{\beta}K_{\beta}^{\alpha} + \nu K_{\alpha}^{\alpha}K_{\beta}^{\beta}\right] \tag{9}$$

The relationship between the membrane stresses, the strain tensor $E_{\alpha\beta}$ and the residual stresses σ is

$$N^{\alpha\beta} = \frac{Eh}{1-\nu^2}\left[(1-\nu)E^{\alpha\beta} + \nu a^{\alpha\beta}E_{\gamma}^{\gamma}\right] - a^{\alpha\beta}\sigma h \tag{10}$$

where $a_{\alpha\beta}$ are the covariant components of the fundamental metric tensor of the surface.

Two dimensionless parameters involving the curvature of the substrate appears for a spherical substrate namely the ratio between the radius of the sphere and the thickness of the film, R/h, and the width, b, of the delamination over the square root of the product between the radius and the thickness, $b/(Rh)^{1/2}$. Numerical results obtained in [8] showed that R/h has an insignificant influence on the energy release rate compared to $b/(Rh)^{1/2}$.

In Fig. 5 a plot of the normalised energy release rate is shown for a spherical substrate as a function of normalised stress in the film for three different values of $b/(Rh)^{1/2}$ and a flat substrate where $b/(Rh)^{1/2} = 0$. It is seen that the curvature drastically increases the energy release rate and thus the probability of delamination especially at low stress levels.

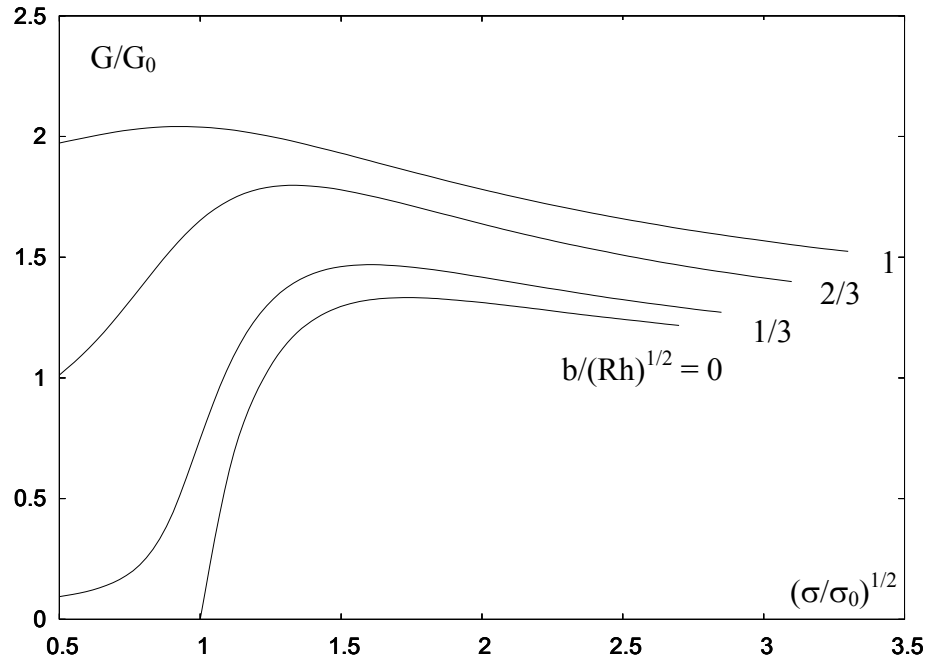

Figure 5. Normalised energy release rate as a function of normalised residual stress for spherical substrate.

The parameters chosen for normalising the energy release rate and residual stress in Fig. 5 are defined as

$$\sigma_0 = \frac{\pi^2 E h^2}{12 b^2 (1-\nu^2)} \quad , \quad G_0 = \frac{(1-\nu^2)h}{2E}\sigma^2 \tag{11}$$

Qualitatively the effect of the substrate curvature is similar to the effect of geometrical imperfections as studied initially in Storåkers and Nilsson [9].

Morphology of buckling driven delamination

Examples of buckling driven delaminations are shown in Fig. 6 (taken from Moon et al. [10]). Especially the telephone cord mode of delamination in Fig. 6(c) has received much attention since it is the most commonly observed mode of delamination.

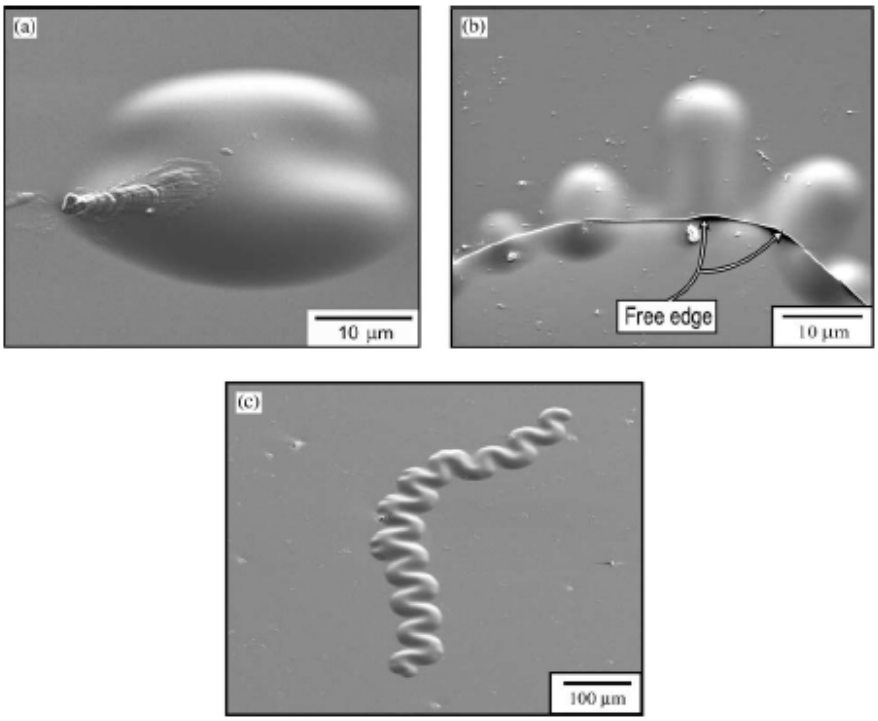

Figure 6. Shapes of bucking driven delamination, (a) circular, (b) straight sided, (c) telephone cord delamination.

The mechanism for the telephone cord delamination suggested in Jensen and Sheinman [11] and supported by the experimental results in [10] is that steady state buckling driven delaminations which propagate along a curved path rather than a straight path release most energy at high stress levels. The cross over point for the two mechanisms of delamination growth lies roughly at $\sigma/\sigma_c = 4$. It was also found in [10] that the straight sided and telephone cord delaminations only exist in a narrow range of mechanical parameters for the thin film system, which separates two regions where either no delamination or complete delamination of the film occurs. The two main parameters for determining whether complete or no delamination occurs is the ratio between the mode I and mode II interface fracture toughness and the total energy per unit area in the film normalised by the mode II fracture toughness.

References

1. H.M. Jensen, J.W. Hutchinson and K.-S. Kim, Decohesion of a Cut Prestressed Film on a Substrate. *International Journal of Solids and Structures* **26**, 1099-1114, 1990.

2. Z. Suo and J.W. Hutchinson, Interface Crack between Two Elastic Layers. *International Journal of Fracture* **43**, 1-18, 1990.

3. H.M. Jensen, Thin Film Delamination at Edges and Corners. *International Symposium on Recent Developments in the Modelling of Rupture in Solids*, (Eds. A. Benallal and S.P.B. Proença), ISBN 2-1-094072-7, 2003.

4. I. Pane and H.M. Jensen, Steady-State Delamination of Thin Films at Corners (in preparation), 2004.

5. J.W. Hutchinson and Z. Suo, Mixed Mode Cracking in Layered Materials. *Advances in Applied Mechanics* **29**, 63-191, 1992.

6. H.M. Jensen and I. Sheinman, Straight-Sided, Buckling-Driven Delamination of Thin Films at High Stress Levels. *International Journal of Fracture* **110**, 371-385, 2001.

7. J.W. Hutchinson, Delamination of Compressed Films on Curved Substrates. *Journal of the Mechanics and Physics of Solids* **49**, 1847-1864, 2001.

8. K.D. Sørensen and H.M. Jensen, Effects of Substrate Curvature on Buckling-Driven Delamination (in preparation), 2004.

9. B. Storåkers and K.F. Nilsson, Imperfection Sensitivity at Delamination Buckling and Growth. *International Journal of Solids and Structures* **30**, 1057-1074, 1993.

10. M.-W. Moon, H.M. Jensen, J.W. Hutchinson, K.H. Oh and A.G. Evans. The Characterization of Telephone Cord Buckling of Compressed Thin Films on Substrates. *Journal of the Mechanics and Physics of Solids* **50**, 2355-2377, 2002.

11. H.M. Jensen and I. Sheinman, Numerical Analysis of Buckling-Driven Delamination. *International Journal of Solids and Structures* **39**, 3373-3386, 2002.